Regeneration of hyaline cartilage promoted by xenogeneic mesenchymal stromal cells embedded within elastin-like recombinamer-based bioactive hydrogels

David Pescador[1,2], Arturo Ibáñez-Fonseca[3,4], Fermín Sánchez-Guijo[1,5], Jesús G. Briñón[1,6], Francisco Javier Arias[3], Sandra Muntión[1,5], Cristina Hernández[7], Alessandra Girotti[3], Matilde Alonso[3], María Consuelo del Cañizo[1,5], José Carlos Rodríguez-Cabello[3*], Juan Francisco Blanco[1,2]

[1] Instituto de Investigación Biomédica de Salamanca (IBSAL), Salamanca, Spain

[2] Servicio de Traumatología y Cirugía Ortopédica. Hospital Universitario de Salamanca, Salamanca, Spain

[3] BIOFORGE Lab, Universidad de Valladolid, CIBER-BBN, Valladolid, Spain

[4] Technical Proteins Nanobiotechnology (TPNBT), Valladolid, Spain

[5] Unidad de Terapia Celular. Servicio de Hematología. Hospital Universitario de Salamanca, Salamanca, Spain

[6] Departamento de Biología Celular y Patología. Universidad de Salamanca, Salamanca, Spain

[7] Servicio de Radiodiagnóstico. Hospital Virgen de la Concha de Zamora, Zamora, Spain

1   *Corresponding author:

2   Prof. J.C. Rodríguez-Cabello

3   roca@bioforge.uva.es

4   BIOFORGE (Group for Advanced Materials and Nanobiotechnology)

5   University of Valladolid

6   Edificio LUCIA

7   Paseo de Belén, 19

8   47011 – Valladolid

9   SPAIN

10   Running Title:

11   Osteochondral regeneration by hMSC-containing ELR-based hydrogels

12   Author Contributions:

13   FJA, FSG, MA, JCRC and JFB were involved in the conception and design of the study,

14   data analysis and interpretation, and in the critical revision for important intellectual

15   content. DP, AIF, AG, JGB and CH performed data acquisition, analysis and

16   interpretation, and were also involved in drafting the article or revising it critically for

17   important intellectual content. FSG, SM and MCdC collected and processed samples

1 from donors, while AG, FJA, MA and JCRC provided essential materials for the study.

2 All authors have read and approved the final submitted manuscript.

3 **ABSTRACT**

4 Over the last decades, novel therapeutic tools for osteochondral regeneration have arisen

5 from the combination of mesenchymal stromal cells (MSCs) and highly specialized

6 smart biomaterials, such as hydrogel-forming elastin-like recombinamers (ELRs), which

7 could serve as cell-carriers. Herein, we evaluate the delivery of xenogeneic human

8 MSCs (hMSCs) within an injectable ELR-based hydrogel carrier for osteochondral

9 regeneration in rabbits. First, a critical-size osteochondral defect was created in the

10 femora of the animals and subsequently filled with the ELR-based hydrogel alone or

11 with embedded hMSCs. Regeneration outcomes were evaluated after three months by

12 gross assessment, magnetic resonance imaging and computed tomography, showing

13 complete filling of the defect and the *de novo* formation of hyaline-like cartilage and

14 subchondral bone in the hMSC-treated knees. Furthermore, histological sectioning and

15 staining of every sample confirmed regeneration of the full cartilage thickness and early

16 subchondral bone repair, which was more similar to the native cartilage in the case of

17 the cell-loaded ELR-based hydrogel. Overall histological differences between the two

18 groups were assessed semi-quantitatively using the Wakitani scale and found to be

19 statistically significant ($p < 0.05$). Immunofluorescence against a human mitochondrial

20 antibody three months post-implantation showed that the hMSCs were integrated into

21 the *de novo* formed tissue, thus suggesting their ability to overcome the interspecies

22 barrier. Hence, we conclude that the use of xenogeneic MSCs embedded in an ELR-

1 based hydrogel leads to the successful regeneration of hyaline cartilage in osteochondral

2 lesions.

3 **KEYWORDS**

4 hyaline cartilage; human mesenchymal stromal cells; elastin-like recombinamers;

5 osteochondral regeneration; xenotransplantation

6

1 INTRODUCTION

2 Osteochondral injuries are a frequent source of pain and disability and can even result in

3 secondary osteoarthritis.[1,2] This disease has an enormous economic impact in developed

4 countries, mostly due to ageing.[3,4] One of the main issues in this regard is that articular

5 cartilage possesses limited regeneration ability due to its avascularity and the cellular

6 and interstitial structure that sustains the biomechanical requirements of joints.[5] As

7 such, it is easy to understand the efforts of orthopedic surgeons in developing novel

8 therapies in this field.[6]

9 The development of novel tissue-engineering methods[7,8] involving mesenchymal

10 stromal cell (MSC) therapy in combination with highly specialized biomaterials has

11 opened up a broad field for the study of articular cartilage regeneration.[9] MSCs are

12 pluripotent cells that can easily be isolated and expanded *in vitro*. Furthermore, these

13 cells can differentiate into diverse cell types (including chondrocytes and osteocytes)

14 and exert immunomodulatory properties, which makes them good candidates for the

15 treatment of musculoskeletal lesions.[10,11] There are different auto-, allo- and xenogeneic

16 sources of MSCs. However, whereas the first two options offer an immunologically

17 safer approach, the latter increases the availability of MSCs enormously. Indeed, there

18 are numerous studies describing the successful use of xenogeneic MSCs in different

19 hosts.[12] Since pre-differentiated cells have been proposed to induce immunological

20 reactions in xenotransplantation models,[13] differentiation may be induced *in vivo* in the

21 presence of some specific endogenous factors in the niche where MSCs are

22 implanted.[14,15]

In contrast, the application of a single suspension of MSCs may lead to poor retention and viability of cells,[16,17] therefore the use of scaffolds is highly recommended in order to increase the persistence and engraftment of the implanted cells at the site of injury. To this end, biomaterials that mimic the extracellular matrix (ECM) and acquire a 3D structure that could be re-populated by cells might be very helpful. Such materials should also be compatible with non-invasive techniques, as is the case for injectable hydrogels. Over the last few decades recombinant DNA techniques have proven to be very powerful tools for the development of novel protein biomaterials that are able to self-assemble into different structures, such as hydrogels.[18,19] These biomaterials include elastin-like recombinamers (ELRs),[20] the composition of which is based on repetition of the VPGXG pentapeptide found in natural elastin, in which X (guest residue) can be any amino acid except L-proline. ELRs show thermosensitivity, which is characterized by a temperature known as the transition temperature (Tt), above which ELRs assemble hydrophobically, undergoing a phase transition, whereas they remain soluble at lower temperatures,[21,22] thus permitting a homogeneous embedding of MSCs. These ELR molecules can self-assemble into hydrogels above the Tt, *i.e.*, at physiological temperature, when designed with a very specific composition,[23] thus allowing the use of the cell-scaffold system in arthroscopy or in injectable therapies, where they adopt the shape of the injured tissue. As a result of their recombinant nature, further genetic modification of these ELRs by addition of the well-known RGD cell-adhesion sequence, which promotes specific cell attachment via integrins,[24] leads to an injectable scaffold that provides a cell-friendly environment.

With regard to the tracking of cartilage regeneration, non-invasive imaging techniques that allow patients to be monitored are highly encouraged. Magnetic resonance imaging (MRI) is the most frequently used imaging method for the evaluation of chondral injuries,[25-27] and this technique is complemented with computed tomography (CT) when subchondral bone has also been damaged.[28]

Despite the ability to monitor evolution of the injured tissue *in vivo*, histology is still essential to demonstrate the regenerative potential of novel treatments when tested in animals. In fact, several methods, such as those of O'Driscoll or Wakitani, aim to quantitatively assess articular cartilage repair by microscopic observation, thereby proposing a more efficient approach for the comparison of different therapies.[29]

In this work, we hypothesized that human MSCs (hMSCs) embedded in an ELR-based hydrogel resembling the ECM would be able to regenerate an osteochondral critical-size defect in a xenotransplantation model in rabbits. Herein, we show results from gross assessment, imaging techniques (MRI and 3D CT) and microscopic evaluation using the Wakitani histological scoring system.

MATERIALS AND METHODS

2.1. Ethical approval

All procedures regarding collection of hMSCs specified below were approved by the Ethics Committee of the University Hospital of Salamanca (Spain) and were also in

1   accordance with the Declaration of Helsinki (1975), as revised in 2000. Informed

2   written consent was obtained from all subjects included in the study.

3   All animal experiments were conducted in accordance with the institutional guidelines

4   for the care and use of experimental animals of the University of Salamanca (Spain) in

5   accordance with Directive 2010/63/EU (Resolution Number 2010/2/23).

6   *2.2. Human mesenchymal stromal cell (hMSC) collection*

7   A volume of 5 mL of bone marrow was obtained from six healthy donors (mean age 55

8   years), by conventional iliac crest aspiration, at the University Hospital of Salamanca.

9   Low density mononuclear cells (MNCs) were isolated using a Ficoll-Paque gradient

10 (Biochrom KG, Berlin, Germany) and plated at a cell density of 10^6 MNC/cm^2 on a

11 polystyrene surface in DMEM (Gibco BRL, Paisley, UK) containing 5% platelet lysate,

12 obtained as reported previously.[30] Culture flasks were maintained in a humidified

13 incubator at 37 °C and 5% CO_2, with medium replacement twice a week, removing non-

14 adherent hematopoietic cells. The cell layer was trypsinized at 80% confluence and cells

15 were subcultured at a cell density of $2.5 \cdot 10^3$ MNC/cm^2. Methods and the results of

16 MSC characterization, according to previous studies, are summarized in the

17 Supplementary Material (Supplementary Methods).[31-33]

18 *2.3. ELR design, bioproduction and characterization*

19 The elastin-like recombinamer (ELR) used in this work was genetically engineered as

20 described elsewhere[19] and provided by Technical Proteins Nanobiotechnology (TPNBT)

S.L. (Spain). Briefly, the ELR was recombinantly bioproduced in *Escherichia coli* in a 15-L bioreactor (Applikon Biotechnology, Netherlands) and purified by several cooling and heating purification cycles (Inverse Transition Cycling) following centrifugation. The ELR sequence and its description can be found in the Supplementary Information (Supplementary Methods and Table S-1).

In order to study the stability of the resulting hydrogels, they were formed by dissolving the ELR in cold phosphate buffered saline (PBS, pH 7.4) at a concentration of 75 mg/mL in glass vials, and heated to 37 °C for 15 minutes. Another vial was kept at 4 °C during that time. Both vials were then placed face down and photographs taken for comparison.

2.4. In vivo experimental model

Six male New Zealand white rabbits with an age of 6 months and an average weight of 3.45 kg were used for the creation and treatment of the osteochondral defects. Animals were anesthetized intramuscularly with xylazine (5 mg/kg) and ketamine (35 mg/kg), then both knees were shaved and cleaned. A parapatellar incision of the skin was performed under sterile conditions in order to expose the distal femur. A 4x4 mm full-thickness critical-size osteochondral lesion was created with a drill. The defect was deep enough to reach the osteochondral bone in every case. Immediately afterwards, a cold solution containing $0.5 \cdot 10^6$ hMSCs embedded in 2 mL of the hydrogel solution (75 mg/mL, culture medium) was used to completely fill the defect of the right knee (n = 6), whereas the hydrogel under the same conditions but without cells was placed in the left

knee to serve as control (n = 6). The wound was closed after less than 1 minute, and the hydrogel fully solidified and adapted itself to the surface of the lesion, as confirmed by visual observation, after coming into contact with the animal tissue, at a temperature above the Tt of the ELR. Gentamicin (5 mg/kg) was administered after the surgical procedure to avoid infection. All animals were fed and watered *ad libitum* during the study period and maintained in individual cages.

Animals were euthanized with pentobarbital (120 mg/kg) at three months post-treatment and the distal femora were extracted for further analysis.

2.5. MRI and 3D CT

Whole legs from two animals were used for image collection using a 1.5 Tesla MRI instrument (Signa LX version 9.1, General Electric), with the sequences Oblique 3D Fast Spoiled Gradient Echo (FRPGR) Special and 3D Spoiled Gradient (3D SPGR).

Two other specimens were used for extraction of both femoral condyles for further image analysis using multi-slice helical CT (Aquilion 16, Toshiba, Japan), obtaining axial sequences of 0.5 mm thickness on the bone window and multi-slice 3D reconstructions in the sagittal and coronal planes.

2.6. Histological analysis

Extracted samples were fixed in 4% formaldehyde and 0.2% picric acid in PBS 0.1 M (pH 7.3) at 4 °C. They were subsequently processed as described in the Supplementary Information.

A blind macro- and microscopic analysis was performed on the samples by a trained histologist. Samples from each rabbit (n = 6 for each group) were classified on the basis of their modified Wakitani score[34] (Table S-2, maximum score of 15) and inter-group comparisons were performed using the non-parametric Kruskal–Wallis test, with a p-value < 0.05 indicating statistically significant differences.

To evaluate the survival of human MSCs, a mouse monoclonal antibody against a 65 kD mitochondrial membrane protein specifically expressed in human cells (MAB1273, Millipore) was used, followed by a secondary antibody, namely donkey anti-mouse IgG, conjugated with Cy3 (Jackson Immunoresearch Europe, Ltd., U.K). The combination with 4',6-diamidino-2-phenylindole (DAPI), a fluorescent stain that binds strongly to A-T rich regions in DNA, allowed all nuclei from both human and rabbit cells to be stained, and thus the xenogeneic cells in the regenerated tissue to be observed in comparison with host cells.

Images were taken under similar conditions of exposure and time for every sample, as stated in the Supplementary Information.
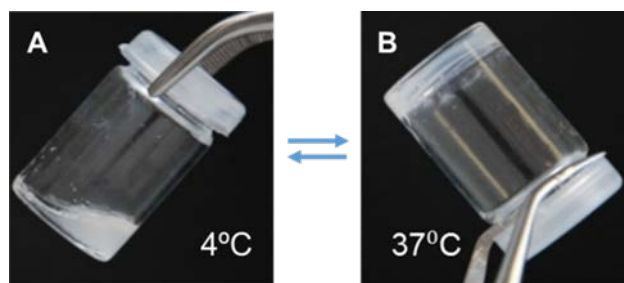
RESULTS

3.1. ELR bioproduction and characterization

The ELR was successfully bioproduced in *E. coli*, purified by ITC and stored lyophilized at -20 °C until further use. The bioproduction yield was found to be an average of 200 mg ELR/L of culture.

1   SDS-PAGE and MALDI-TOF confirmed the purity, integrity and molecular weight of

2   the ELR, which coincided with the theoretical value. Thus, the experimental molecular

3   weight was found to be 112,253 Da, while the theoretical value was 112,270 Da (Figure

4   S-1). Moreover, the Tt was found to be 15.3 °C in PBS (Figure S-2), which means that

5   hydrogels are formed at physiological temperature upon ELR transition. The ^{1}H NMR

6   spectrum (Figure S-3 and Table S-3) and amino acid analysis (Table S-4) showed the

7   absence of contaminants in the final ELR product.

8   To macroscopically assess hydrogel formation, the ELR was dissolved at 4 °C and then

9   warmed to 37 °C. The vial containing the hydrogel was then placed upside-down and

10 the hydrogel found to be formed and stable, in other words it did not fall from the

11 bottom of the tube or dilute in an aqueous solvent (Figure 1).

12

13 **Figure 1.** ELR dissolved at 4 ℃ (A) and hydrogel formed at 37 ℃ (B), inverted to show

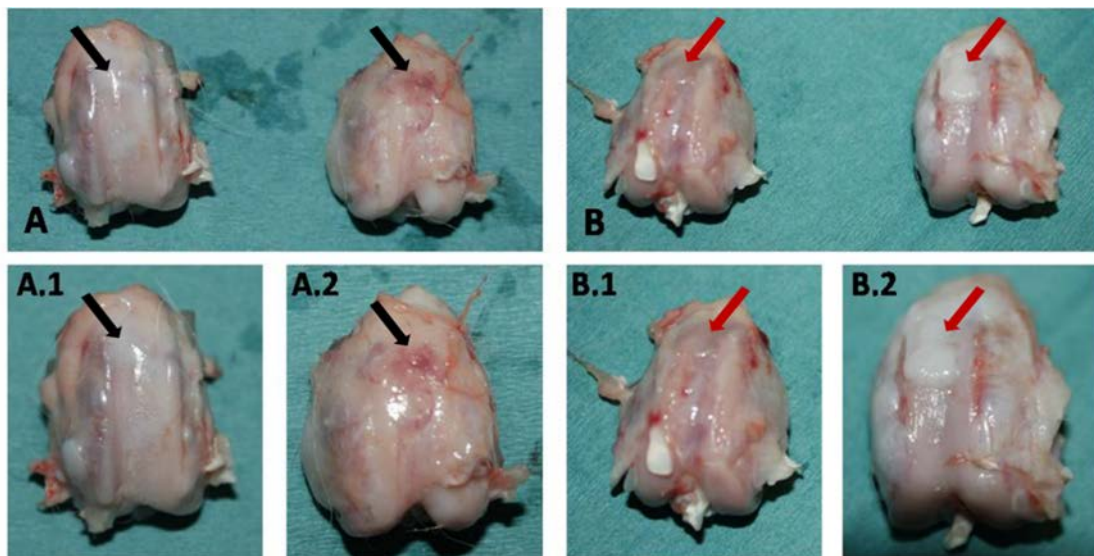14 the hydrogel state and its stability.

15 *3.2. Macroscopic evaluation*

16 A. Control group (ELR)

1   A partially regenerated whitish region could be observed macroscopically in the

2   extracted femora, with this area being paler than the surrounding normal cartilage.

3   Furthermore, the appearance thereof was not smooth and it presented a fibrotic surface,

4   with protrusions (Figure 2, red arrows) projecting slightly from the rest of the articular

5   surface (Figure 2, A2 and B2), thus differing from the appearance of non-injured

6   cartilage.

7   B. Experimental group (ELR + hMSCs)

8   Regenerated tissue with a smooth and bright appearance was observed in all cases. The

9   injured region could be recognized by its more greyish colour in comparison with the

10   regenerated cartilage. Moreover, the regenerated tissue was well integrated into the

11   surrounding chondral tissue, with continuity between the two structures (Figure 2, A1

12   and B1, black arrows), thus resembling the situation found in non-injured cartilage.

13

1   **Figure 2.** Images showing the comparison between femurs extracted from the same

2   animals (A and B) treated either with hMSCs combined with the ELR-based hydrogel

3   (experimental group) (A1, B1), or with the ELR-based hydrogel alone (control group)

4   (A2, B2). Defects are indicated with black and red arrows for the experimental and the

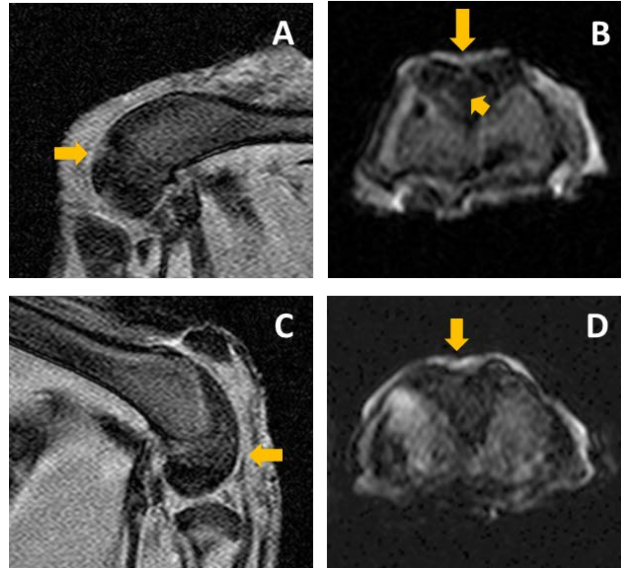5   control group, respectively.

6   *3.3. Image analysis*

7   <u>3.3.1. MRI</u>

8   <u>A. Control group (ELR)</u>

9   The 3D SPGR (Figure 3A) magnetic resonance sequence showed articular cartilage loss

10   (yellow arrow) and an underlying bone oedema of approximately 3 mm along the major

11   axis in both samples studied. Similarly, axial 3D FSPGR (Figure 3B) showed a

12   discontinuity in the articular cartilage of the femoral condyle (long yellow arrow) with

13   underlying bone lesion (short yellow arrow).

14   <u>B. Experimental group (ELR + hMSCs)</u>

15   Regenerated articular cartilage could be observed in all sequences acquired, showing a

16   healthy subchondral bone (3D SPGR, Figure 3C, yellow arrow), while the condyle

17   surface showed no fractures or traces of bone oedema in any case (3D FSPGR, Figure

18   3D, yellow arrow highlighting regenerated defect), thus suggesting complete restoration

19   of the injured tissue in every sample.

1

Figure 3. MRI analysis of femurs extracted from rabbits in the control group (ELR

hydrogel, A and B) and experimental group (ELR hydrogel + hMSCs, C and D). A and

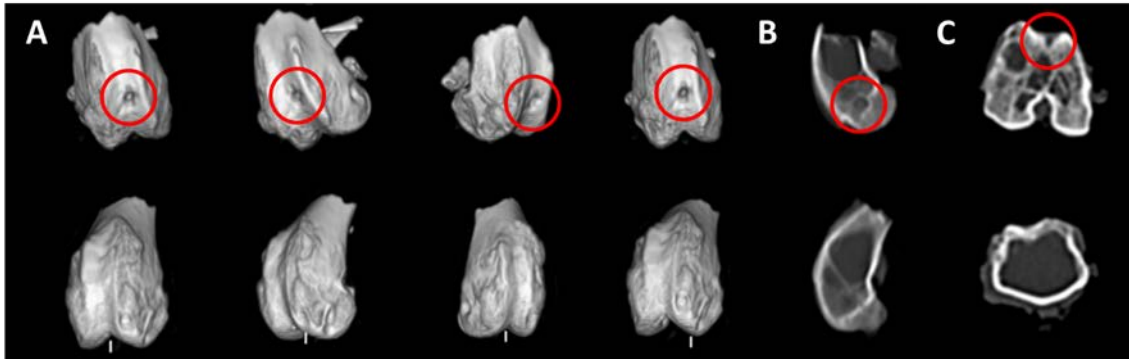C, and B and D correspond to the 3D SPGR and 3D FSPGR sequences, respectively.

3.3.2. 3D CT

A. Control group (ELR)

A 3D reconstruction of the femoral condyles (Figure 4 (top)) showed a bone defect of

up to 3x3 mm in the transverse and anteroposterior planes, with articular cartilage loss,

thus indicating a partially repaired osteochondral lesion (red outlines). These findings

were confirmed in the sagittal and axial plane images (Figure 4B and C, respectively).

B. Experimental group (ELR + hMSCs)

The osteochondral defect was imperceptible in the specimen from the experimental

group (Figure 4, bottom), thus indicating an almost fully regenerated injury (Figure 4A).

15

Sagittal (Figure 4B) and axial (Figure 4C) plane images corroborated the result found in the 3D reconstruction, thereby also confirming the MRI findings.
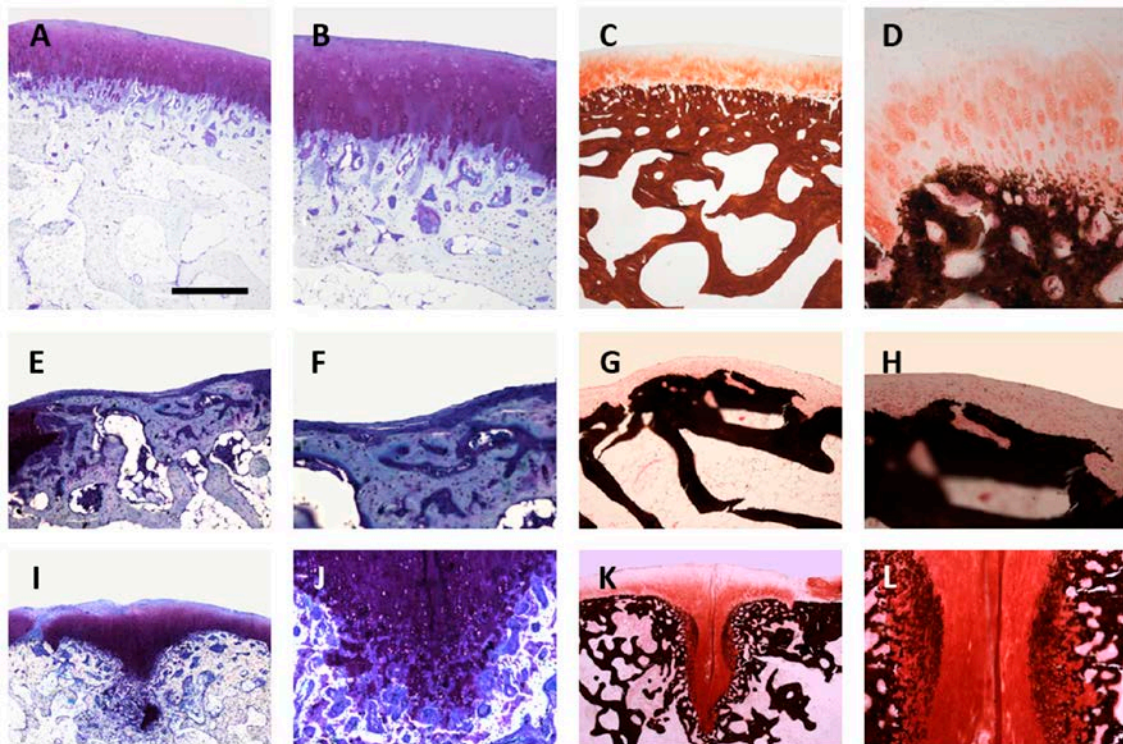

Figure 4. 3D CT reconstructions (A) and sagittal and axial slices (B and C) of femurs from rabbits in the control group (top) and experimental group (bottom). Marked defects are highlighted in red.

3.4. Histological analysis

Toluidine blue stain was used to clarify the distribution of cells and collagen fibres in the extracellular matrix, as well as cell morphology, thus allowing the observation of osteoblasts and osteocytes, together with bone lamellas and bone marrow cells, the cytoplasm of which was stained a deep blue colour. Furthermore, this metachromatic colorant allowed the identification of newly formed bone tissue (stained violet), with the chondral matrix being stained into reddish and purple hues. In addition, Von Kossa staining allowed calcified regions to be differentiated from other tissue by its dark brown colour.

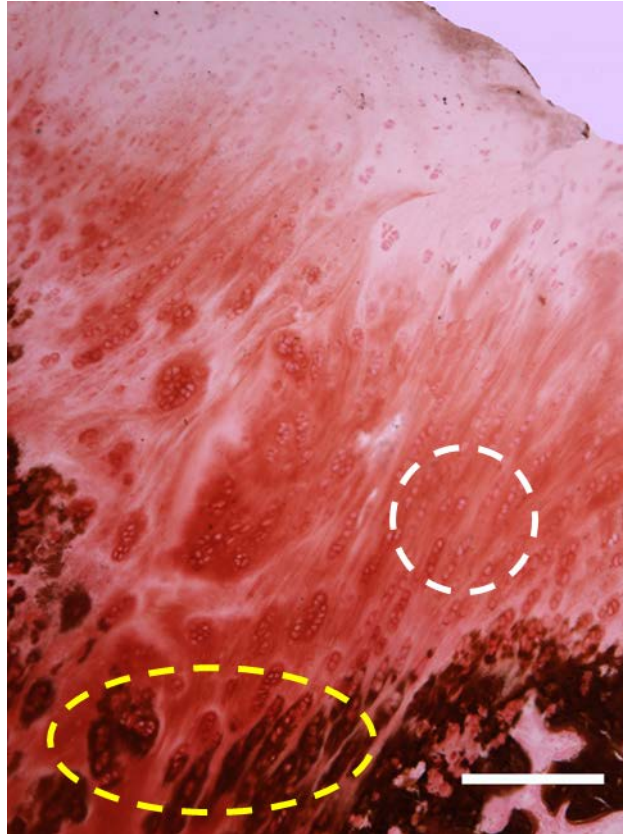1   <u>3.4.1. Microscopic evaluation</u>

2   The regenerated tissue at the articular surface of samples from the control group

3   exhibited a minimal thickness in comparison with adjacent non-injured articular

4   cartilage (Figure 5). Moreover, this tissue showed a fibrotic appearance, similar to the

5   features of fibrocartilage, arranged on a base of subchondral bone trabeculae that is

6   mostly regenerated. This fibrocartilage-like tissue was composed of small egg-shaped

7   cells, the major axis of which was oriented parallel to the articular surface, following the

8   orientation of the fibres that compose the matrix in which the cells are embedded.

9   However, this tissue was not found to be integrated with the surrounding hyaline

10   cartilage present at the surface of non-injured cartilage.

11

Figure 5. Toluidine blue (left) and Von Kossa (right) staining of non-injured tissue (A-D) and samples from the control (ELR, E-H) and experimental groups (ELR + hMSCs, I-L). Scale bar corresponds to 1 mm for I and K, 500 μm for A and C, 250 μm for B, D, E, G, J and L, and 125 μm for F and H.

In contrast, coronal sections from samples from the experimental group (ELR + hMSCs) showed the osteochondral defect area to be entirely filled with a tissue identified as hyaline cartilage. This regenerated cartilage displayed a smooth and regular surface and was completely integrated with the adjacent non-injured cartilage, with no signs of discontinuity in any case. The different layers comprising *de novo* formed cartilage could also be clearly observed, showing no structural differences with respect to healthy cartilage. The defect in the subchondral bone beneath the regenerated articular cartilage was filled with a tissue with the structural and staining features of cartilage. Regions of hypertrophied chondrocytes could be found towards the edges of the cartilage near the subchondral bone, and the neighbouring matrix was moderately calcified, which was identified as an endochondral ossification process. These areas continued to the edges of the injured zone until they reached trabeculae from intact bone tissue, with no interruption with the adjacent bone. Filling of cartilaginous tissue was observed in the bone area of the lesion. A further demonstration of these results can be seen in Figure 6, in which a well regenerated articular cartilage (white outline) can be seen together with ossification areas below it (yellow outline), showing a similar structure to that found in native osteochondral tissue.
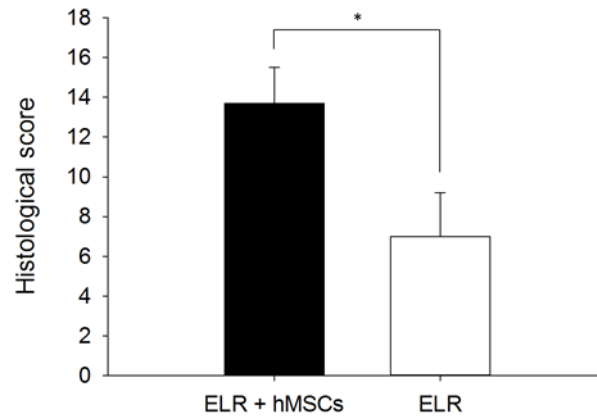
Figure 6. Von Kossa staining of a sample from the experimental group showing complete regeneration of articular cartilage (white dotted line) with areas of ossification (yellow dotted line) beneath the cartilage. Scale bar corresponds to 250 μm.

3.4.2. Histological evaluation using the modified Wakitani grading scale

A statistical blind study of the histological sections using the modified Wakitani scale gave a total score of 13.7 points for the defects from the experimental group (ELR + hMSCs), which is close to the score for healthy cartilage (15 points). In contrast, evaluation of the defects from the control group (ELR) gave a score of 7 points, with a statistically significant difference (p < 0.01) in the overall score between experimental

1 and control groups (Figure 7). Complete scores from the histological evaluation are
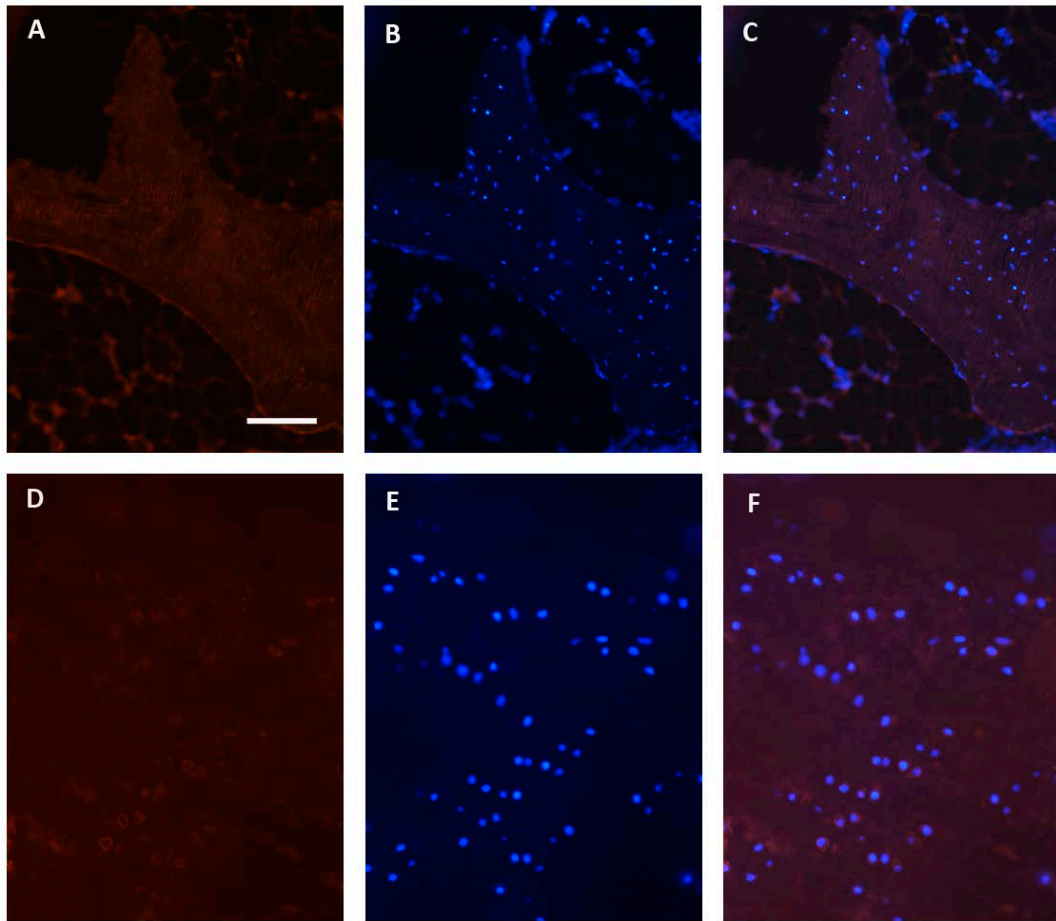
2 shown in Table S-5 (Supplementary Material).

3

4 **Figure 7.** Comparison between the histological scores obtained for the experimental

5 (ELR + hMSCs) and control (ELR) groups, according to the modified Wakitani scale

6 (*p < 0.01).

7 3.4.3. Immunofluorescence analysis

8 The immunofluorescence results, obtained by combining antibodies versus the human

9 mitochondrial marker (red) and DAPI staining (blue), showed that hMSCs were

10 involved in regeneration of the osteochondral defect, since cells have a chondrocyte-like

11 morphology and arrangement, integrating the *de novo* formed tissue. This was only

12 observed in sections from the experimental group, with no fluorescence being detected

13 in the control group (Figure 8).

Figure 8. Immunofluorescence images to human mitocondrial marker, in red (A, D), DAPI, in blue (B, E), an merged images (C, F) taken from animals of the control group (ELR, A-C) and the experimental group (ELR + hMSC, D-E) showing the presence of hMSCs in the regenerated tissue of animals from the experimental group. Scale bar = 125 μm for A-C, and 50 μm for D-F.

DISCUSSION

We have described the use of MSCs encapsulated within an ELR-based hydrogel to regenerate an osteochondral defect for the first time. Although there are previous studies

1 regarding the treatment of this type of lesions with ELRs, none of them included any

2 type of cells inside the scaffold, and the outcomes observed were not very promising,

3 being similar to those for the control group.[35,36] Furthermore, both studies involved the

4 use of chemically cross-linked hydrogels, which makes them harder to handle and may

5 lead to toxic sub-products. Moreover, in one case the ELR-based hydrogel was not

6 formed *in situ*, which compromises the adaptability to the shape of the defect, and the

7 use of genipin as cross-linker increases the expense considerably.[35] In our case the

8 network sustaining the hydrogel is formed via physical cross-linking (hydrophobic

9 interactions) above the Tt, e.g., at physiological temperature. As such, this system is

10 highly suitable for non-invasive techniques due to its injectability below the Tt. In

11 addition, biofunctionalization of the ELR by the genetic fusion of a 12-mer peptide

12 containing the RGD cell-adhesion sequence provides a cell-friendly environment for

13 hMSCs.

14 This approach represents a significant advance in the regeneration of osteochondral

15 injuries because it is widely thought that biomaterials should simulate the properties of

16 cartilage and subchondral bone, thus requiring biphasic[37] or even triphasic[38] scaffolds

17 that must comprise biomaterials with different features to recapitulate the osteochondral

18 interface and promote healing. However, here we show that the use of an injectable

19 ELR-based single hydrogel is an efficient approach in regenerative medicine as this

20 biomaterial serves only as a temporary microenvironment and does not need to have the

21 same properties as the native tissues.[39]

1 Regeneration of the injured cartilage was successfully studied using a 1.5T MRI

2 instrument, without contrast agents, similarly to analogous models.[40,41] This study

3 showed almost complete regeneration of the damaged tissue in the experimental group

4 (ELR + hMSCs) after three months. It was also possible to study the development of

5 subchondral bone with high precision by CT, thereby demonstrating regeneration of the

6 tissue and emphasizing the importance of this procedure for assessing regeneration of

7 osteochondral injuries in combination with MRI. This may allow more invasive

8 methods, such as biopsy, to be avoided.[42]

9 With respect to the histological findings, the experimental (ELR + hMSCs) and control

10 (ELR) groups obtained 13.7 and 7 points, respectively, on the Wakitani scale, at three

11 months post-implantation. We chose this grading scale due to its simplicity in

12 comparison to other systems. Taking into account that the maximum score on this scale

13 is 15 points (Table S-2), we can calculate the percentage regeneration as the ratio

14 between the obtained and maximum values. Thus, we obtained a value of 91% for the

15 experimental group and 47% for the control group. This means that we can compare the

16 outcomes of osteochondral regeneration with MSCs (auto-, allo- or xenotransplanted),

17 at the same timepoint (3 months), even when different grading scales and/or animal

18 models are used, especially when considering that regeneration may vary between

19 species. For instance, Nakamura *et al*. created an osteochondral defect in both legs of

20 pigs, subsequently treating one knee with allogeneic MSCs while leaving the other as a

21 control. Their results, according to the same histological scoring scale as used in our

22 work, showed 57% regeneration for the experimental joint and 10% regeneration for the

control joint.[34] In another study, Koga *et al*. implanted allogeneic MSCs within a collagen scaffold in rabbit knees, with the collagen hydrogel alone as control. Their histological scoring (unmodified Wakitani scale) gave a regeneration of 89% and 21% for the experimental and control groups, respectively.[43] Similarly, Mazaki *et al*. described the use of allogeneic MSCs embedded in a gelatin hydrogel, obtaining 66% regeneration in this case and 42% when using the gelatin hydrogel alone (modified ICRS scale).[44]

Other hydrogels have also been used in osteochondral regeneration. For instance, Miller *et al*. studied the ability of an injectable peptide hydrogel combined with chondrogenic factors and allogeneic MSCs to regenerate an osteochondral defect in rabbits, finding poorer repair when MSCs were included in the hydrogel.[45] For their part, D'Este *et al*. evaluated an injectable thermoresponsive hyaluronan/pNIPAAm hydrogel in an analogous system, but not including MSCs. Their results showed better regeneration in the non-treated (75%) than in the hydrogel-treated defects (70%).[46] Although these authors claim that this biomaterial is biocompatible and does not interfere with the intrinsic healing response, its implantation does not result in an improvement and thus it is not very likely to be accepted by clinicians. In another study, Levingstone *et al*. demonstrated the use of collagen-based scaffolds combined with other biomaterials (multi-phasic scaffold) to recapitulate the osteochondral interface, without including MSCs.[47] They reported 80% regeneration of defects treated with the cited scaffold, as opposed to the 44% observed in the control non-treated defects. In contrast, Pulkkinen *et al*. observed no significant differences in terms of histological assessment between

1 treatment of an osteochondral defect with recombinant human type II collagen

2 hydrogels embedding autologous chondrocytes and the spontaneously repaired tissue.[48]

3 In the light of all these comparisons (see Table S-6, Supplementary Information), we

4 can conclude that our preliminary study represents a novel non-invasive therapy for the

5 treatment of injuries affecting articular cartilage with very promising results that are

6 better than those found in the literature in every case. One of the reasons that could

7 explain the differences between our study and others is the use of a bioactive ELR-

8 based hydrogel containing RGD cell-adhesion sequences, which therefore serves as an

9 ECM-like vehicle for hMSCs and provides a cell-friendly environment that supports

10 their regenerative potential. However, due to the subjectivity of histological scoring,

11 particular care must be taken when drawing conclusions from a direct comparison of the

12 results from different studies.

13 It is important to highlight the xenogeneic nature of the animal model used in this study.

14 This kind of cell therapy has been proposed as a replacement for allogeneic and

15 autologous bone and cartilage implantation, which have some limitations, especially a

16 shortage of donor tissue and the time-consuming nature of the procedure. Xenogeneic

17 MSCs have been used as undifferentiated cells, such as in our study, showing better

18 regeneration outcomes and higher survival than differentiated hMSCs.[13,49] However,

19 Jang *et al.* showed good regeneration (75%) when including chondrocyte-differentiated

20 hMSCs in a biphasic composite (hydroxyapatite and platelet-rich fibrin glue) scaffold.[50]

21 Similarly, the literature review by Li *et al*. concluded that porcine MSCs downregulate

22 T cell responses *in vitro*, which could also be reproduced *in vivo*, hence being a feasible

approach in clinical applications.[12] In contrast, Pei *et al*. reported a detrimental effect of xenotransplanted MSCs in comparison to their non-treated control.[14] In this case, we believe that the influence of the matrix used as cell carrier was not considered as a source of this effect and should be studied in more detail.

Moreover, the use of xenogeneic hMSCs allowed us to track the implanted cells in the articular cartilage of the rabbit using a novel immunofluorescence technique that involves the use of an antibody towards a specific human mitochondrial marker, thus discerning between transplanted and host cells. This method allowed us to detect viable and engrafted hMSCs after three months, thus proving that the ELR-based hydrogel can be used as a successful cell carrier in which cells can differentiate and regenerate damaged tissue. Our results therefore confirm that MSCs can overcome inter-species barriers. In addition, we observed that the implanted human cells show a chondrocyte-like shape and arrangement, similar to that of native cartilage, thus suggesting that differentiation into a chondral cell lineage has taken place, which is in good agreement with previous findings by Koga *et al*.[43]

In summary, this work shows the potential effectiveness of a tissue-engineering approach for regeneration of a critical-size osteochondral defect, in terms of morphology and structure, upon combining hMSCs with a recombinantly developed ELR-based cell-carrier hydrogel. The comparison with other approaches found in the literature shows a more hyaline-like regeneration, and the closest previous result (89%, by Koga *et al*.) involves the use of a non-injectable scaffold, which limits its application in non-invasive therapies. This system provides a bioactive scaffold in which cells may

be embedded for accurate delivery to the injury site to promote tissue-engineered regeneration of native-like hyaline cartilage. Further studies will be performed to evaluate the functionality of regenerated articular cartilage through biomechanical tests, and to determine the biochemical composition of the repaired tissue before translating this system into larger animal models or humans.

ACKNOWLEDGMENTS

CONFLICT OF INTERESTS

The authors have no competing interests to declare.

REFERENCES

1.   Bhosale AM, Richardson JB. 2008. Articular cartilage: structure, injuries and review of management. Br Med Bull 87:77-95.

2.   Kuettner KE, Cole AA. 2005. Cartilage degeneration in different human joints. Osteoarthritis Cartilage 13:93-103.

3. Maetzel A, Li LC, Pencharz J, et al. 2004. The economic burden associated with osteoarthritis, rheumatoid arthritis, and hypertension: a comparative study. Annals of the rheumatic diseases 63:395-401.

4. Hiligsmann M, Reginster J-Y. 2013. The economic weight of osteoarthritis in Europe. Medicographia 35:197-202.

5. Chevalier X. 1998. Physiopathology of arthrosis. The normal cartilage. . Presse Med 27(2):75-80.

6. Pei M, Yan Z, Shoukry M, et al. 2010. Failure of xenoimplantation using porcine synovium-derived stem cell-based cartilage tissue constructs for the repair of rabbit osteochondral defects. J Orthop Res 28:1064-1070.

7. Kerker JT, Leo AJ, Sgaglione NA. 2008. Cartilage repair: synthetics and scaffolds: basic science, surgical techniques, and clinical outcomes. Sports Medicine and Arthroscopy 16:208-216.

8. Vaquero J, Forriol F. 2011. Knee chondral injuries: Clinical treatment strategies and experimental models. Injury.

9. Bartlett W, Gooding CR, Carrington RW, et al. 2005. Autologous chondrocyte implantation at the knee using a bilayer collagen membrane with bone graft. A preliminary report. The Journal of bone and joint surgery British volume 87:330-332.

10. Chen F, Rousche K, Tuan R. 2006. Technology Insight: adult stem cells in cartilage regeneration and tissue engineering. Nature Clinical Practice Rheumatology 2(7):373-382.

11. Kessler M, Ackerman G, Dines J, et al. 2008. Emerging technologies and fourth generation issues in cartilage repair. Sports Medicine and Arthroscopy 16(4):246-254.

12. Li J, Ezzelarab MB, Cooper DKC. 2012. Do mesenchymal stem cells function across species barriers? Relevance for xenotransplantation. Xenotransplantation 19:273-285.

13. Niemeyer P, Vohrer J, Schmal H, et al. 2008. Survival of human mesenchymal stromal cells from bone marrow and adipose tissue after xenogenic transplantation in immunocompetent mice. Cytotherapy 10:784-795.

14. Pei M, Yan Z, Shoukry M, et al. 2010. Failure of xenoimplantation using porcine synovium-derived stem cell-based cartilage tissue constructs for the repair of rabbit osteochondral defects. Journal of Orthopaedic Research 28:1064-1070.

15. Revell CM, Athanasiou KA. 2009. Success rates and immunologic responses of autogenic, allogenic, and xenogenic treatments to repair articular cartilage defects. Tissue Engineering Part B Reviews 15:1-15.

16. Roche ET, Hastings CL, Lewin SA, et al. 2014. Comparison of biomaterial delivery vehicles for improving acute retention of stem cells in the infarcted heart. Biomaterials 35:6850-6858.

17. Martens TP, Godier AFG, Parks JJ, et al. 2009. Percutaneous Cell Delivery Into the Heart Using Hydrogels Polymerizing In Situ. Cell transplantation 18:297-304.

18.   Girotti A, Orbanic D, Ibáñez-Fonseca A, et al. 2015. Recombinant Technology in the Development of Materials and Systems for Soft-Tissue Repair. Advanced Healthcare Materials 4:2423-2455.

19.   Rodriguez-Cabello JC, Girotti A, Ribeiro A, et al. 2012. Synthesis of genetically engineered protein polymers (recombinamers) as an example of advanced self-assembled smart materials. Methods in molecular biology 811:17-38.

20.   Rodriguez-Cabello JC, Martin L, Girotti A, et al. 2011. Emerging applications of multifunctional elastin-like recombinamers. Nanomedicine (London, England) 6:111-122.

21.   Urry DW. 1993. Molecular Machines - How Motion and Other Functions of Living Organisms Can Result from Reversible Chemical-Changes. Angewandte Chemie-International Edition in English 32:819-841.

22.   Tamburro AM, Guantieri V, Pandolfo L, et al. 1990. Synthetic fragments and analogues of elastin. II. Conformational studies. Biopolymers 29:855-870.

23.   Martin L, Arias FJ, Alonso M, et al. 2010. Rapid micropatterning by temperature-triggered reversible gelation of a recombinant smart elastin-like tetrablock-copolymer. Soft Matter 6:1121-1124.

24.   Ruoslahti E, Pierschbacher MD. 1986. Arg-Gly-Asp: A versatile cell recognition signal. Cell 44:517-518.

25.   Caumo F, Russo A, Faccioli N, et al. 2007. Autologous chondrocyte implantation: prospective MRI evaluation with clinical correlation. La radiologia medica 112:722-731.

26. Marlovits S, Striessnig G, Resinger CT, et al. 2004. Definition of pertinent parameters for the evaluation of articular cartilage repair tissue with high-resolution magnetic resonance imaging. European Journal of Radiology 52:310-319.

27. Trattnig S, Millington SA, Szomolanyi P, et al. 2007. MR imaging of osteochondral grafts and autologous chondrocyte implantation. European Radiology 17:103-118.

28. Barber FA, Dockery WD. 2011. A computed tomography scan assessment of synthetic multiphase polymer scaffolds used for osteochondral defect repair. Arthroscopy 27:60-64.

29. Orth P, Zurakowski D, Wincheringer D, et al. 2011. Reliability, Reproducibility, and Validation of Five Major Histological Scoring Systems for Experimental Articular Cartilage Repair in the Rabbit Model. Tissue Engineering Part C: Methods 18:329-339.

30. Pérez-Simon JA, López-Villar O, Andreu EJ, et al. 2011. Mesenchymal stem cells expanded in vitro with human serum for the treatment of acute and chronic graft-versus-host disease: results of a phase I/II clinical trial. Haematologica 96:1072-1076.

31. Villaron E, Almeida J, Lopez-Holgado N, et al. 2004. Mesenchymal stem cells are present in peripheral blood and can engraft after allogeneic hematopoietic stem cell transplantation. Haematologica 89:1421-1427.

1 32. Conget PA, Minguell JJ. 1999. Phenotypical and functional properties of human

2   bone marrow mesenchymal progenitor cells. Journal of Cellular Physiology

3   181:67-73.

4 33. Beyer Nardi N, da Silva Meirelles L. 2006. Mesenchymal stem cells: isolation,

5   in vitro expansion and characterization. Handbook of experimental

6   pharmacology:249-282.

7 34. Nakamura T, Sekiya I, Muneta T, et al. 2012. Arthroscopic, histological and

8   MRI analyses of cartilage repair after a minimally invasive method of

9   transplantation of allogeneic synovial mesenchymal stromal cells into cartilage

10   defects in pigs. Cytotherapy 14:327-338.

11 35. Hrabchak C, Rouleau J, Moss I, et al. 2010. Assessment of biocompatibility and

12   initial evaluation of genipin cross-linked elastin-like polypeptides in the

13   treatment of an osteochondral knee defect in rabbits. Acta Biomaterialia 6:2108-

14   2115.

15 36. Nettles DL, Kitaoka K, Hanson NA, et al. 2008. In Situ Crosslinking Elastin-

16   Like Polypeptide Gels for Application to Articular Cartilage Repair in a Goat

17   Osteochondral Defect Model. Tissue Engineering Part A 14:1133-1140.

18 37. Schütz K, Despang F, Lode A, et al. 2016. Cell-laden biphasic scaffolds with

19   anisotropic structure for the regeneration of osteochondral tissue. Journal of

20   Tissue Engineering and Regenerative Medicine 10:404-417.

21 38. Marquass B, Somerson JS, Hepp P, et al. 2010. A novel MSC-seeded triphasic

22   construct for the repair of osteochondral defects. Journal of Orthopaedic

23   Research 28:1586-1599.

39. Yang J, Shrike Zhang Y, Yue K, et al. Cell-Laden Hydrogels for Osteochondral and Cartilage Tissue Engineering. Acta Biomaterialia.

40. Kangarlu A, Gahunia HK. 2006. Magnetic resonance imaging characterization of osteochondral defect repair in a goat model at 8 T. Osteoarthritis Cartilage 14:52-62.

41. Kim M, Foo LF, Uggen C, et al. 2010. Evaluation of early osteochondral defect repair in a rabbit model utilizing fourier transform-infrared imaging spectroscopy, magnetic resonance imaging, and quantitative T2 mapping. Tissue Engineering Part C Methods 16:355-364.

42. Haleem AM, Singergy AA, Sabry D, et al. 2010. The Clinical Use of Human Culture-Expanded Autologous Bone Marrow Mesenchymal Stem Cells Transplanted on Platelet-Rich Fibrin Glue in the Treatment of Articular Cartilage Defects: A Pilot Study and Preliminary Results. Cartilage 1:253-261.

43. Koga H, Muneta T, Ju YJ, et al. 2007. Synovial stem cells are regionally specified according to local microenvironments after implantation for cartilage regeneration. Stem Cells 25:689-696.

44. Mazaki T, Shiozaki Y, Yamane K, et al. 2014. A novel, visible light-induced, rapidly cross-linkable gelatin scaffold for osteochondral tissue engineering. Scientific Reports 4:4457.

45. Miller RE, Grodzinsky AJ, Vanderploeg EJ, et al. 2010. Effect of self-assembling peptide, chondrogenic factors, and bone marrow-derived stromal cells on osteochondral repair. Osteoarthritis and Cartilage 18:1608-1619.

1   46.   D'Este M, Sprecher CM, Milz S, et al. 2016. Evaluation of an injectable

2   thermoresponsive hyaluronan hydrogel in a rabbit osteochondral defect model.

3   Journal of Biomedical Materials Research Part A 104:1469-1478.

4   47.   Levingstone TJ, Thompson E, Matsiko A, et al. 2016. Multi-layered collagen-

5   based scaffolds for osteochondral defect repair in rabbits. Acta Biomaterialia

6   32:149-160.

7   48.   Pulkkinen HJ, Tiitu V, Valonen P, et al. 2013. Repair of osteochondral defects

8   with recombinant human type II collagen gel and autologous chondrocytes in

9   rabbit. Osteoarthritis and Cartilage 21:481-490.

10 49.   Liu S, Jia Y, Yuan M, et al. 2017. Repair of Osteochondral Defects Using

11   Human Umbilical Cord Wharton's Jelly-Derived Mesenchymal Stem

12   Cells in a Rabbit Model. BioMed Research International 2017:12.

13 50.   Jang K-M, Lee J-H, Park CM, et al. 2014. Xenotransplantation of human

14   mesenchymal stem cells for repair of osteochondral defects in rabbits using

15   osteochondral biphasic composite constructs. Knee Surgery, Sports

16   Traumatology, Arthroscopy 22:1434-1444.